2026 IEEE International Conference on Robotics and Automation (ICRA 2026)
June 1-5, 2026. Vienna, Austria

GenJAPNet: A Generalizable Joint Angle Prediction Network with Non-Redundant Muscle Synergy Features for Lower-Limb Exoskeletons

Hairong Zhang[1], Yu Bai[1], Ziming Kou[2], Juan Wu[2], Pengjie Qin[3], Fei Gao[4], Wenze Shang[4], Yue Teng[4], Dingkui Tian[4,*], Xinyu Wu[4], *Fellow, IEEE*

***Abstract*— Lower-limb exoskeleton robots play a significant role in both rehabilitation and assisted walking, where accurate prediction of lower-limb joint angles is crucial for achieving natural gait. However, due to inter-subject variability and differences across locomotion modes, achieving cross-task generalization in joint angle prediction remains a major challenge. This work proposes a novel framework for multi-joint angle prediction in the lower-limb, which includes a non-redundant muscle synergy feature extraction algorithm and a Generalizable Joint Angle Prediction Network (GenJAPNet) across speeds and subjects. The feature extraction algorithm employs Non-negative Matrix Factorization (NMF) to extract activation coefficient matrix from Surface Electromyography (sEMG) signals, followed by further dimensionality reduction using Uniform Manifold Approximation and Projection (UMAP) to obtain more discriminative and non-redundant features. GenJAPNet leverages pre-trained shared features and few-shot fine-tuning to rapidly adapt to new task. Through feature extraction algorithm comparison experiments, cross-speed and cross-subject experiments, and exoskeleton-assisted walking physical experiments, the effectiveness and generalizability of this method are validated, demonstrating its potential for enhancing the performance of lower-limb exoskeleton rehabilitation and assistive applications.**

I. Introduction

Lower-limb exoskeleton robots play a vital role in assisted walking, rehabilitation training, and daily functional enhancement. They not only help patients with impaired lower-limb mobility regain basic walking ability but also provide elderly individuals with movement support, thereby improving quality of life and independence [1]. As a key component of exoskeleton control, accurate joint angle prediction is essential, and improvements in prediction performance directly drive the advancement and application of exoskeleton technology [2]. Surface electromyography (sEMG) reflects neuromuscular activation and, compared with optical motion capture, offers advantages such as non-invasiveness and wearability. Moreover, sEMG activity typically precedes kinematic and kinetic signals [3], making it widely adopted for human motion intention prediction, particularly in joint angle estimation [4], [5].

Raw sEMG signals are often noisy and high-dimensional, which can degrade model performance and robustness. Hence, feature extraction is typically employed to distill representative features prior to modeling. Turner et al. [6] extracted eight Time-Domain (TD) features from sEMG signals and applied them to five machine learning models. The results showed that the Willison Amplitude feature consistently achieved the best performance across all models. Moslhi et al. [7] proposed two Time-Frequency Domain (TFD) feature extraction methods, one based on the Fast Fourier Transform and the other on wavelet transform. Li et al. [8] proposed a discrete wavelet transform-based data alignment method for sEMG signals, which reduces the distribution discrepancy between the source and target domains by decomposing, reorganizing, and reconstructing the TFD signals. TFD features extracted from sEMG signals capture signal intensity and spectral distribution but fail to represent the coupling control of multiple muscles by the central nervous system. Moreover, methods such as wavelet decomposition often produce a large number of features, many of which are similar or redundant.

Unlike TFD features, muscle synergy features reflect how the Central Nervous System (CNS) coordinates multiple muscles through different synergy patterns [9], [10], offering strong physiological interpretability. Non-negative Matrix Factorization (NMF) is a widely used method for extracting muscle synergy features [11], [12]. Lv et al. [13] employed NMF to extract activation coefficient matrices and muscle synergy matrices from sEMG signals for spatiotemporal feature modeling, thereby enabling continuous prediction of hip and knee joint angles. Ma et al. [14] proposed a muscle synergy extraction method based on constrained NMF to address the local optimal solution problem of the standard NMF algorithm. However, due to the strong correlation among multi-channel sEMG signals and the inherent redundancy of motor control, the decomposed muscle synergy features often contain redundant information. To address this issue,

*This work was supported in part by the National Natural Science Foundation of China under Grants 62373346, 62125307, and 62403453; in part by the Shenzhen Science and Technology Program under Grants JCYJ20250604182958078, KJZD20230923113801004, and KJZD20230923115215032; and in part by the Guangdong Provincial Key Laboratory of Multimodality Non-Invasive Brain-Computer Interfaces under Grant 2024B1212010010.

[1]Hairong Zhang and Yu Bai are with Changchun University of Science and Technology, changchun 130000, China. (e-mail: 2023100766@mails.cust.edu.cn, baiyu@cust.edu.cn).

[2]Ziming Kou and Juan Wu are with Taiyuan University of Technology, Taiyuan 030600, China. (e-mail: kouziming@tyut.edu.cn, wujuanz@163.com).

[3]Pengjie Qin is with School of Artificial Intelligence, Shenzhen University, Shenzhen 518060, China (e-mail:pj.qin@szu.edu.cn).

[4]Fei Gao, Wenze Shang, Yue Teng, XinyuWu, Dingkui Tian are with Shenzhen Institutes of Advanced Technology, Chinese Academy of Sciences, Shenzhen 518055, China. (e-mail: gaofeicsu104@gmail.com, shangwenze@gmail.com, y.teng@siat.ac.cn, ,dk.tian1@siat.ac.cn; xy.wu@siat.ac.cn).

*Corresponding author: Dingkui Tian.

Qin and Lu et al. [15], [16] performed cosine similarity analysis on the decomposed activation coefficient matrix and distinguished redundant from non-redundant features based on the similarity levels. However, this approach relies on the manual selection of threshold values. In addition, Zhao et al. [17] combined Empirical Mode Decomposition with Kernel Principal Component Analysis to extract non-redundant key features from sEMG signals. However, the absence of non-negativity constraints limits the physiological interpretability of this approach.

Establishing the mapping from sEMG signals and their extracted features to joint angles is the core of joint angle prediction, and deep learning models have been widely employed in this task due to their powerful nonlinear modeling capabilities. Wei et al. [18] proposed a hybrid 3DCNN-Transformer neural network, which frames the prediction of joint angles from sEMG signals as a sequence-to-sequence translation problem, thereby achieving rapid and accurate joint angle estimation. Huang et al. [19] proposed a Pathfinder-based Long Short-Term Memory network with an attention mechanism, which optimizes weight allocation to significantly enhance the accuracy of joint angle prediction. Zhou et al. [20] proposed a hierarchical spiking attentional feature decomposition network, which employs a spiking sparse attention encoder and a spiking attentional feature decomposition module to compress and decompose sEMG signals, thereby effectively reducing the inference cost of joint angle prediction. Although the aforementioned models achieve accurate joint angle prediction, their strong dependence on the individual characteristics of the training data limits their adaptability to unseen subjects or novel movement patterns. To address this issue, Lin et al. [21] proposed a rotary Transformer model based on Adversarial Transfer Learning for continuous estimation of joint movements across subjects. Du et al. [22] proposed a meta-transfer learning framework that integrates multiple modalities, enabling the model to rapidly adapt to new individuals with only a few training samples. Such transfer learning approaches can effectively address cross-subject adaptation issues. However, achieving rapid adaptation to different movement speeds and individual subjects within a single framework remains a critical challenge for practical exoskeleton applications.

As illustrated in Fig. 1, this study proposes a generalizable framework for lower-limb multi-joint angle prediction, which comprises a non-redundant muscle synergy feature extraction algorithm and a joint angle prediction model capable of cross-speed and cross-subject generalization. In the feature extraction stage, sEMG signals are first decomposed via NMF to obtain the activation coefficient matrix, which is then reduced in dimensionality using Uniform Manifold Approximation and Projection (UMAP) to eliminate redundant information. The angle prediction model consists of a Residual Network (ResNet) layer, three Temporal Convolutional Network - Bidirectional Long Short-Term Memory (TCN-BiLSTM) modules, and a meta-learner, designed to capture local features, spatiotemporal dependencies, and aggregate information. Experiments on our self-built dataset demonstrate that the non-redundant muscle synergy features are effective through feature comparison, the framework achieves generalization across different speeds and subjects, and its feasibility is validated through physical exoskeleton walking experiments. Our main contributions are:

- A non-redundant muscle synergy feature extraction algorithm is proposed. The algorithm extracts physiologically interpretable and discriminative features from sEMG signals, demonstrating superior performance compared to TD features.
- A Generalizable Joint Angle Prediction Network (GenJAPNet) with cross-speed and cross-subject adaptability is developed. By extracting shared features through pre-training and leveraging few-shot fine-tuning, the network can rapidly adapt to new task.
- The effectiveness and generalization capability of the proposed method is validated through feature comparison experiment, cross-speed and cross-subject experiments, and physical walking experiments with the exoskeleton.

II. Method

We propose a novel framework that extracts non-redundant muscle synergy features from sEMG signals and achieves multi-joint angle prediction of the lower limbs across walking speeds and subjects through a pretraining and fine-tuning strategy based on a meta-learner. The effectiveness of our method is further validated through experiments on a four-degree-of-freedom exoskeleton robot.

A. A Neural Activation Non-redundant Feature Extraction Algorithm Based on NMF-UMAP

During feature extraction, NMF-UMAP is employed to derive non-redundant muscle synergy features from sEMG signals. Specifically, NMF is first applied to extract the activation coefficient matrix that reflects human motor control patterns. The resulting activation coefficients are then reduced in dimensionality using the nonlinear embedding method UMAP, yielding lower-dimensional, more stable, and discriminative feature representations.

NMF. The sEMG signal ($V_{n\times t}$) is decomposed by NMF into a basis matrix ($W_{n\times k}$) and an activation coefficient matrix ($H_{k\times t}$), where the basis matrix represents the contribution of each muscle in different muscle synergy modes, and the activation coefficient matrix represents the activation degree of each synergy mode at different times.

$$V_{n\times t} = W_{n\times k} \cdot H_{k\times t} \tag{1}$$

where n denotes the number of sEMG channels, t denotes the length of the time series, and k denotes the number of muscle synergies.

UMAP. Due to the strong correlation between different collaboration modes and certain features that reflect noise and individual differences, the activation coefficient matrix ($H_{k\times t}$) obtained from NMF decomposition often contains redundant information. UMAP is a nonlinear dimensionality

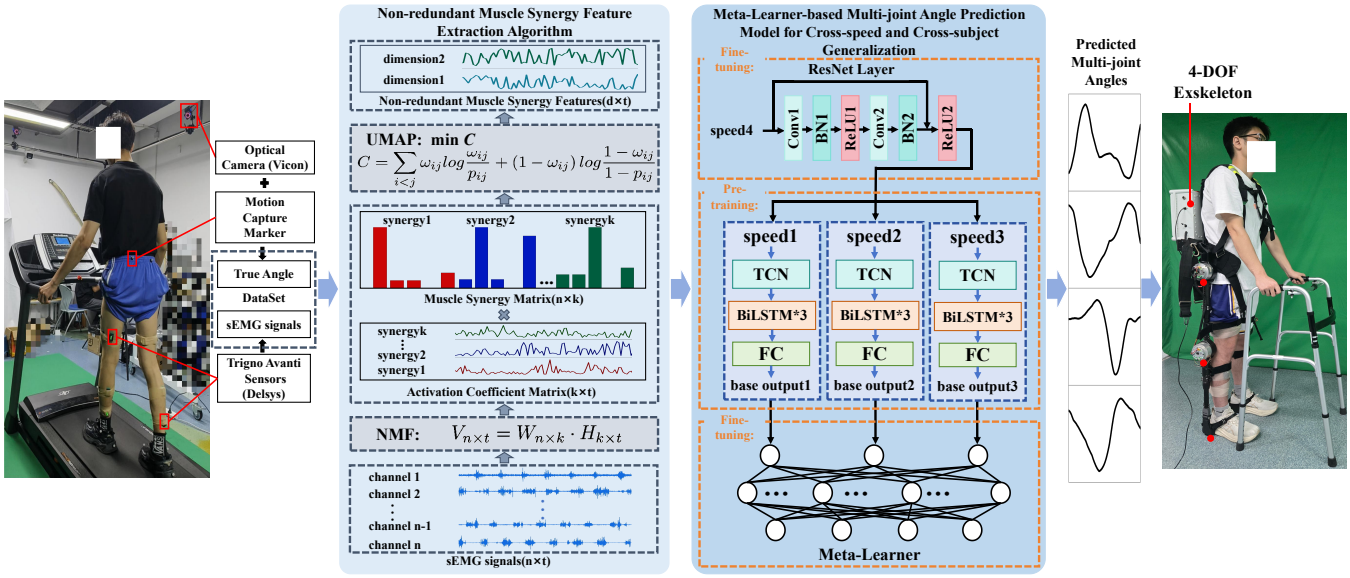

Fig. 1: Pipeline of the proposed method, including data acquisition, non-redundant muscle synergy feature extraction, multi-joint angle prediction across speeds and subjects, and exoskeleton validation.

reduction technique that approximates the manifold structure of high-dimensional data and projects it into a low-dimensional space, preserving local neighborhood relationships while maintaining the global distribution. In order to extract more discriminative features, UMAP was used to reduce the dimensionality of the activation coefficient matrix ($H_{k\times t}$), thereby obtaining non-redundant muscle synergy features($x_{d\times t}$, $d < k$).

$$x_{d\times t} = UMAP(H_{k\times t}) \tag{2}$$

where d denotes the number of feature dimensions after dimension reduction of the activation coefficient matrix H.

B. Structure of the Meta-learner-based Multi-joint Angle Prediction Model

Non-redundant muscle synergy features are extracted using NMF-UMAP, then processed using a sliding window with a window size of 300 and a step size of 10, as input for the angle prediction model. The main components of our model include multiple TCN-BiLSTM modules for pre-training to extract general features, a ResNet layer and a meta-learner for fine-tuning to adapt to new tasks with few samples.

ResNet Layer. The ResNet layer is composed of two convolutional layers with a kernel size of 3, two batch normalization layers, and two ReLU activation functions, along with a residual connection. The residual connection adds the input to the output of the convolutional block and forwards the sum to the subsequent module.

TCN-BiLSTM Module. We designed a TCN-BiLSTM module consisting of a TCN network, three stacked BiLSTM layers, and a fully connected layer. The TCN contains three spatio-temporal convolution blocks, each containing two expansion causal convolution layers with a kernel size of 3 and a residual connection. The final fully connected layer maps the extracted features to the output space.

Meta-learner. The features extracted from the ResNet layer are fed into three parallel TCN-BiLSTM modules, yielding three separate prediction results. A meta-learner [23], implemented as a fully connected neural network with three layers and two intermediate ReLU activations, is then employed to integrate the outputs of the three TCN-BiLSTM modules. By treating the combined predictions as new high-level features, the meta-learner further refines the representation and generates the final joint angle prediction.

C. Training Strategy

The proposed training strategy consists of two phases: pre-training and fine-tuning.

Pre-training Phase. In this phase, data from three walking speeds are used to train the three parallel TCN-BiLSTM modules. After feature extraction, the non-redundant muscle synergy feature corresponding to each speed are individually fed into one TCN-BiLSTM module, enabling each module to learn distinct initial parameters. This phase allows the TCN-BiLSTM modules to capture generalizable temporal features across different walking speeds.

Fine-tuning Phase. During fine-tuning, the parameters of the three pre-trained TCN-BiLSTM modules are frozen, while the ResNet layer and the meta-learner are updated. For a novel walking speed or a new subject, the model does not require extensive data for training. Effective adaptation can be achieved with only about 30% of the data. The input features are first processed by the ResNet layer to extract local features, which are then passed into the three pre-trained TCN-BiLSTM modules to obtain three base predictions. The meta-learner integrates these predictions and generates the final joint angle output, thereby achieving robust adaptation across speeds or subjects.

For example, in the cross-speed experiment, the model is pre-trained using data from Subject S1 at walking speeds of 1.0, 2.0, and 3.0 km/h. Fine-tuning is then conducted with a limited amount of data at 1.5 km/h, demonstrating the model's ability to generalize to unseen speeds with few samples.

III. Experiments and Results

A. Data Acquisition and Preprocessing

sEMG signals and hip and knee joint angle data were collected from three healthy subjects walking at six different speeds of 1.0, 1.5, 2.0, 2.5, 3.0 and 3.5 km/h. Similarly, limited data from the lower-limb muscle-injured Subject S4 were collected in the same manner. During data collection, electromyography electrodes were attached to eight major muscles in the lower limbs of each subject, including the rectus femoris, tibialis anterior, vastus medialis, vastus lateralis, biceps femoris, semitendinosus, gastrocnemius, and soleus. The sEMG signals were recorded via Trigno avanti sensors (Delsys, USA). Hip and knee angles were captured by the VICON motion capture system. Sixteen marker points were attached to the lower limbs of each subject to construct the Plug-in Gait Lower Body Model. During movement, the X, Y, and Z coordinates of each marker point were collected, and after completion, the joint angles of the hip and knee joints were calculated using the dynamic model. Trigno avanti sensors collect sEMG signals at a frequency of 1000 Hz, while the VICON system collects joint angle data at a frequency of 100 Hz. The two data collection devices are synchronized in time via triggering.

To avoid noise interference in the collected data, perform data preprocessing. First, check the data for non-finite values, then remove the DC offset from each sEMG signal. Next, apply a 4th-order Butterworth bandpass filter (20 Hz–450 Hz) to the sEMG signal to remove low-frequency motion artifacts and high-frequency noise, followed by full-wave rectification. Then, use a 4th-order Butterworth low-pass filter (6 Hz) to extract the signal envelope, and finally downsample to 100 Hz to align with the joint angle.

B. Comparison of Feature Extraction Algorithms

To validate the effectiveness of the proposed non-redundant muscle synergy feature extraction algorithm, a feature comparison experiment was conducted. Different features were extracted using different feature extraction algorithms, and then these features were used as inputs to the model. The effectiveness of the features was evaluated by comparing the performance of the model in predicting hip and knee joint angles. The model used here is a TCN with three temporal convolution modules and a convolution kernel size of 3. Other feature extraction algorithms obtain TD features such as Mean Absolute Value (MAV), Root Mean Square (RMS), and Waveform Length (WL) from sEMG signals.

The number of muscle synergies in NMF and the target dimensionality in UMAP are two key parameters in the proposed feature extraction algorithm. These parameters are optimized through grid search. The base model is a TCN with three temporal convolution modules and a convolution kernel size of 3. The number of muscle synergies in NMF ranges from 1 to 8. For each value, the sEMG signals are decomposed to obtain the activation coefficient matrix, which is then used as input for the base model to predict joint angles. The Correlation Coefficient (CC) of predicted hip and knee joint angles is computed for all cases. Experimental results show that the best prediction performance is achieved when the number of muscle synergies is 8. The target dimensionality of UMAP is varied from 2 to 8, and for each dimensionality, the activation coefficient matrix from NMF decomposition with 8 synergies is reduced to lower dimensions, producing non-redundant features as input for the base model. The Root Mean Square Error (RMSE) of predicted angles is computed for all cases. Experimental results show that the best performance is achieved when the target dimensionality is 5.

As shown in the Table I, these are the average values of the predicted results obtained by all subjects using different feature extraction methods at six walking speeds. At nearly all walking speeds and joints, the predictive performance of the NMF-UMAP feature extraction algorithm outperforms other algorithms, demonstrating the effectiveness of NMF-UMAP in extracting non-redundant muscle synergy features. For example, at a walking speed of 1.0 km/h, the RMSE of NMF-UMAP on the right hip is 3.0567°, which is 15.73% lower than NMF's 3.6274° and 29.61% lower than MAV's 4.3427°, a 30.95% reduction compared to RMS's 4.4268°, and a 52.03% reduction compared to WL's 6.3726°.

C. Generalization Across Speeds and Subjects

Cross-speed experiments and cross-subject experiments were conducted to verify the generalizability and effectiveness of the proposed method. At the same time, other baseline methods were conducted as comparison in the cross-speed experiments. To verify the effectiveness of knowledge transfer in cases with a small number of samples, experiments were conducted in which models were constructed directly using the small number of sample data for prediction, and these were compared with cross-subject experiments.

Experimental Setup of Cross-speed Experiments. For Subjects S1, S2, S3, three TCN-BiLSTM modules are pre-trained using input features at walking speeds of 1.0, 2.0, and 3.0 km/h, respectively, and their parameters are subsequently frozen. Fine-tuning is then performed on the ResNet layer and the meta-learner using limited samples from 1.5, 2.5, and 3.5 km/h. In the comparative experiments, four advanced models, including Quantile-Regression, Temporal Convolutional Network-Bidirectional Long Short-Term Memory(QRTCN-BiLSTM) [24], Convolutional Neural Network (CNN)-LSTM-Attention [25], Informer [26], and Nonlinear AutoRegressive with eXogenous inputs(NARX) [27] based on the Gated Recurrent Unit(GRU) model, were selected as baseline methods.

Experimental Setup of Cross-subject Experiments. In the cross-subject experiments, three TCN-BiLSTM modules

TABLE I: Feature Extraction Algorithms Performance Comparison

Algorithms	Speeds (km/h)	RMSE(°)				CC			
		Left Hip	Left Knee	Right Hip	Right Knee	Left Hip	Left Knee	Right Hip	Right Knee
MAV	1.0	4.5673	5.5694	4.3427	5.6782	0.8783	0.9251	0.8864	0.9133
	1.5	5.1701	7.5898	5.7605	8.6019	0.8725	0.8446	0.7451	0.7645
	2.0	4.2408	6.4594	4.3225	6.1945	0.9291	0.9296	0.9189	0.9366
	2.5	3.9730	5.9402	4.1752	6.9829	0.9439	0.9477	0.9412	0.9356
	3.0	4.1932	6.3526	4.4278	6.2854	0.9432	0.9496	0.9349	0.9486
	3.5	3.3339	5.1777	3.5740	5.7987	0.9696	0.9651	0.9670	0.9649
RMS	1.0	4.7293	5.6308	4.4268	5.5702	0.8730	0.9252	0.8844	0.9193
	1.5	6.0607	8.1772	5.9698	8.6185	0.6823	0.7687	0.6474	0.7527
	2.0	4.4471	6.4915	4.6360	6.8246	0.9198	0.9281	0.9063	0.9193
	2.5	4.0659	5.9496	4.2352	6.9235	0.9398	0.9465	0.9400	0.9363
	3.0	4.0229	**5.9846**	4.2301	**5.8008**	0.9511	**0.9557**	0.9417	0.9572
	3.5	3.3672	5.0191	3.5941	5.6901	0.9690	0.9673	0.9655	0.9655
WL	1.0	6.1175	8.2851	6.3726	8.8494	0.7668	0.8172	0.6999	0.8000
	1.5	5.1691	7.8533	5.0224	7.6018	0.8642	0.8541	0.8808	0.9059
	2.0	4.9376	7.4763	4.9872	7.8522	0.8957	0.9029	0.9046	0.9034
	2.5	4.6916	6.4653	4.9652	7.8901	0.9207	0.9361	0.9200	0.9234
	3.0	4.3759	6.9306	4.1238	5.9360	0.9416	0.9360	0.9475	0.9526
	3.5	3.9849	5.8957	4.2980	6.2446	0.9575	0.9556	0.9510	0.9578
NMF	1.0	3.6929	6.5414	3.6274	5.0681	0.9038	0.8890	0.9254	0.9292
	1.5	3.4300	5.2209	3.6314	5.2381	0.9452	**0.9531**	0.9369	0.9511
	2.0	3.4752	5.4847	2.7780	5.4373	0.9481	0.9472	0.9694	0.9572
	2.5	**2.5128**	**4.8495**	2.4661	3.6326	0.9782	**0.9661**	0.9789	0.9811
	3.0	2.9031	6.1156	3.4736	6.0972	0.9724	0.9533	0.9677	0.9634
	3.5	2.2668	3.8301	2.2855	2.9472	0.9847	0.9832	0.9882	0.9917
NMF-UMAP	1.0	**3.2490**	**4.8373**	**3.0567**	**4.7406**	**0.9310**	**0.9407**	**0.9466**	**0.9421**
	1.5	**3.1387**	**5.0269**	**3.1238**	**4.4569**	**0.9535**	0.9529	**0.9524**	**0.9624**
	2.0	**3.1378**	**5.4686**	**2.4320**	**5.1289**	**0.9569**	**0.9489**	**0.9767**	**0.9636**
	2.5	2.5524	5.4079	**2.2273**	**3.3602**	**0.9790**	0.9579	**0.9820**	**0.9855**
	3.0	**2.8899**	6.2608	**3.1033**	5.8307	**0.9748**	0.9465	**0.9751**	**0.9684**
	3.5	**1.9574**	**3.3517**	**1.9975**	**2.8119**	**0.9885**	**0.9852**	**0.9899**	**0.9941**

are pre-trained using input features of S1 at walking speeds of 1.0, 2.0, and 3.0 km/h, respectively, and their parameters are subsequently frozen. Fine-tuning is then performed on the ResNet layer and the meta-learner using limited samples from the remaining subjects S2, S3, S4 at 1.5, 2.5, and 3.5 km/h. Without knowledge transfer, the model architecture was modified to adapt to few-shot data. A simplified hybrid TCN-BiLSTM module,comprising two temporal convolutional blocks and a single BiLSTM layer,is employed, with the meta-learner input adjusted accordingly, while keeping the other components unchanged.

Results of cross-speed and Cross-subject Experiments. As shown in Fig. 2, the proposed method achieves superior performance in cross-speed joint angle prediction compared to baseline models. Specifically, our method achieved the lowest RMSE across all four joints, with average values of 1.8494°, 2.7904°, 1.7031°, and 2.4519° for the left hip, left knee, right hip, and right knee, respectively. The corresponding average CC values were 0.9872, 0.9877, 0.9891, and 0.9907. These results indicate that our approach ensures more accurate and stable joint angle prediction across different joints. Moreover, based on the distribution of data points in the figure, our method yields more concentrated prediction results, indicating superior stability and generalization capabilities. Statistical significance tests indicate that the improvements of our method over the baselines are highly significant. These results validate the effectiveness of the proposed framework in addressing the challenges of cross-speed joint angle prediction.

As illustrated in Fig. 3, our method consistently outperforms the baseline model without knowledge transfer in the cross-subject experiment. For the left hip, left knee, right hip, and right knee joints, the mean RMSEs of the proposed method were 2.2160°, 3.4507°, 2.2470°, and 3.2376°, respectively, with mean CC values all exceeding 0.98. Additionally, the smaller error bars in our method indicate that the experimental results are more concentrated, demonstrating greater stability in this approach. In most cases, the statistical significance p-values were all less than 0.001, validating that the proposed knowledge transfer strategy effectively enhances cross-object generalization capabilities and significantly improves prediction accuracy and reliability.

D. Experimental Validation on a Four-DOF Robot

To further validate the effectiveness of the proposed method, physical experiments were conducted using a four-degree-of-freedom exoskeleton robot actuated by the bilateral hip and knee joints. The predicted gait of Subject S3 was obtained through the cross-speed experiment using his own data. For Subject S4, the predicted gait was generated via the cross-subject experiment, in which the model was pretrained on S1's data at walking speeds of 1.0, 2.0, and 3.0 km/h, and subsequently fine-tuned using S4's limited data at 1.0,

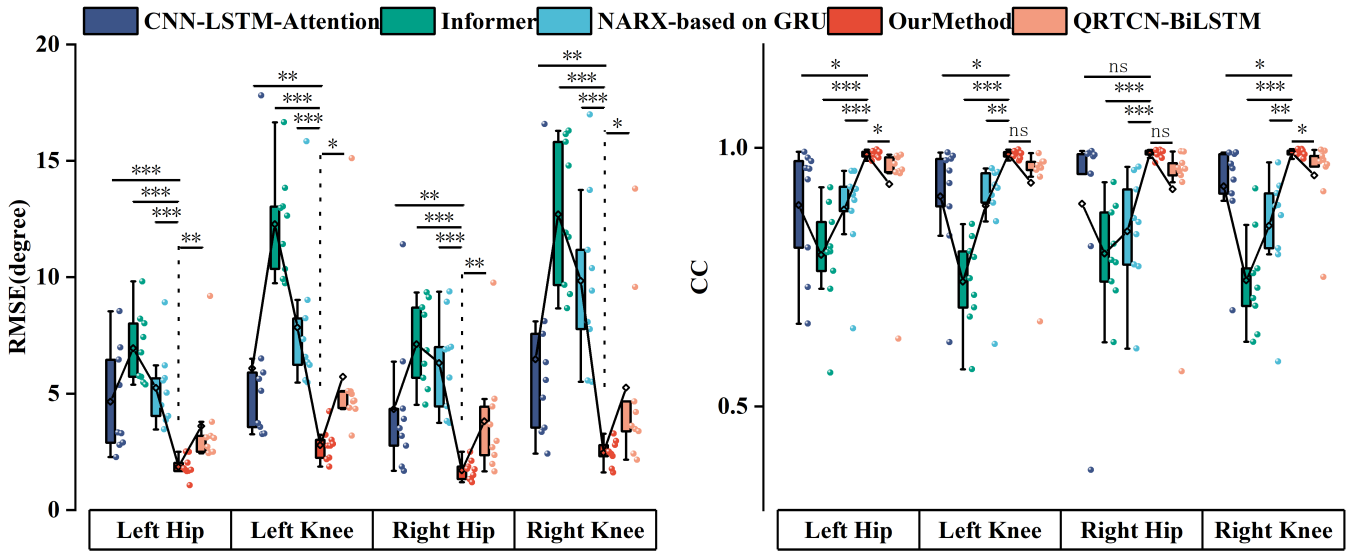

Fig. 2: Box plots of RMSE and CC for multi-joint angle prediction results in cross-speed comparison experiments. Small spheres represent prediction results for three speeds across three subjects, while connecting lines denote average values. ns represents statistical significance p>0.05, * represents p<0.05, ** represents p<0.01, *** represents p<0.001.

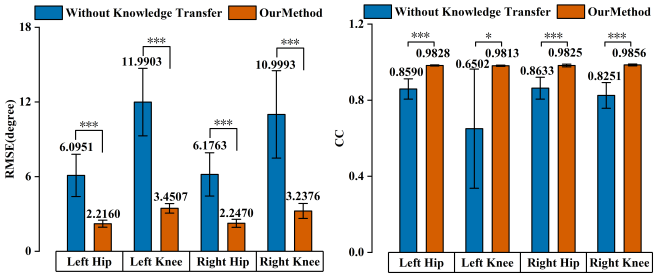

(a) (b)

Fig. 3: Results of cross-subject experiments and experiments without knowledge transfer. The error bars represent the standard deviation of the experimental results. * represents statistical significance p<0.05, ** represents p<0.01, *** represents p<0.001.

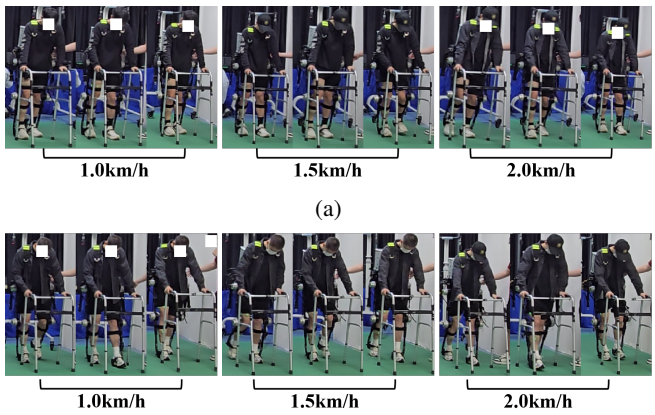

(a)

(b)

Fig. 4: Two subjects walking with an exoskeleton at predicted gait speeds of 1.0, 1.5, and 2.0 km/h. (a) S3 walking under predicted gait in the cross-speed experiment. (b) S4 walking under predicted gait in the cross-subject experiment.

1.5, and 2.0 km/h. As shown in the Fig. 4, both S3 and S4 successfully walked with the exoskeleton under the predicted gait at speeds of 1.0, 1.5, and 2.0 km/h.

As shown in Fig. 5, response gait trajectories of the bilateral hip and knee joints generated when Subject S3 and S4 walked with the exoskeleton at three different speeds. These results demonstrate the reliability of the proposed cross-speed and cross-subject generalized multi-joint angle prediction method, which enables accurate joint angle prediction from limited data and facilitates daily walking tasks for lower-limb muscle-injured subjects using exoskeletons.

IV. Discussion and Conclusion

The comparative results of feature extraction demonstrate that the non-redundant muscle synergy features obtained from sEMG signals via NMF-UMAP outperform conventional TD features (e.g., RMS) as well as muscle synergies extracted directly by NMF in joint angle prediction. This superiority arises because muscle synergy features inherently capture the motor control strategies of the CNS and the coupling relationships among lower-limb muscles, thereby providing strong physiological interpretability. Moreover, by applying dimensionality reduction to the activation coefficient matrix, UMAP effectively suppresses highly similar interference within the synergies, removes redundant information, and yields more discriminative features. However, the effectiveness of NMF-UMAP feature extraction is influenced by key parameters such as the number of muscle synergies and the target dimensionality in the reduction process. Determining these parameters more efficiently and accurately remains an open challenge.

The results of cross-speed and cross-subject experiments

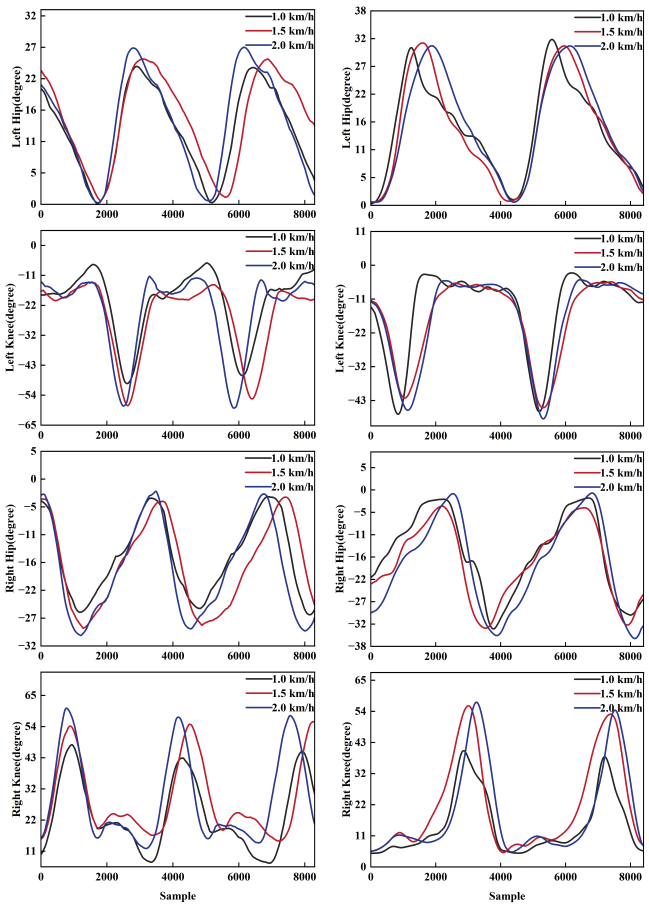

(a) (b)

Fig. 5: Response gaits generated at speeds of 1.0, 1.5, and 2.0 km/h. (a) Response gaits of S3 at speeds of 1.0, 1.5, and 2.0 km/h in the cross-speed experiment. (b) Response gaits of S4 at speeds of 1.0, 1.5, and 2.0 km/h in the cross-subject experiment.

demonstrate that the proposed method outperforms baseline approaches in joint angle prediction, exhibiting strong generalization capability. In the cross-subject setting, compared with baseline methods trained directly on limited samples, pretraining on other subjects' data followed by fine-tuning with few samples proved more effective, validating the advantage of knowledge transfer in addressing the few-shot problem. Specifically, during pretraining, shared features were captured across different speeds or subjects, while in fine-tuning, the meta-learner aggregated three base outputs and retrained to learn how to effectively combine them, thereby enabling rapid adaptation to new tasks and enhancing generalization. Furthermore, the successful execution of predicted gait in exoskeleton walking experiments highlights the applicability of our method to real-world assistive walking. Nevertheless, although the proposed framework alleviates the challenges of generalization and limited data, it still relies on extensive pretraining to acquire sufficient prior knowledge.

In this work, a generalized lower-limb multi-joint angle prediction approach with cross-speed and cross-subject adaptability is proposed. The framework consists of a non-redundant muscle synergy feature extraction algorithm based on neural activation and a meta-learner-based multi-joint angle prediction model. To validate the effectiveness of the proposed method, a series of experiments are conducted. Feature comparison experiments demonstrate that the proposed feature extraction method outperforms conventional TD features. Cross-speed and cross-subject experiments against baseline methods further validate the accuracy and generalization capability of our approach. Finally, physical walking experiments with an exoskeleton executing the predicted gait confirm the effectiveness and reliability of the proposed method. In future work, we will further generalize to more complex motion patterns such as uphill locomotion.

REFERENCES

[1] H. Lee, P. W. Ferguson, and J. Rosen, "Lower limb exoskeleton systems—overview," *Wearable Robotics*, pp. 207–229, 2020.

[2] M. Belal, N. Alsheikh, A. Aljarah, and I. Hussain, "Deep learning approaches for enhanced lower-limb exoskeleton control: A review," *IEEE Access*, vol. 12, pp. 143 883–143 907, 2024.

[3] T. Teramae, T. Noda, and J. Morimoto, "Emg-based model predictive control for physical human–robot interaction: Application for assist-as-needed control," *IEEE Robotics and Automation Letters*, vol. 3, no. 1, pp. 210–217, 2017.

[4] D. Xiong, D. Zhang, X. Zhao, and Y. Zhao, "Deep learning for emg-based human-machine interaction: A review," *IEEE/CAA Journal of Automatica Sinica*, vol. 8, no. 3, pp. 512–533, 2021.

[5] D. Xiong, D. Zhang, Y. Chu, Y. Zhao, and X. Zhao, "Intuitive human-robot-environment interaction with emg signals: A review," *IEEE/CAA Journal of Automatica Sinica*, vol. 11, no. 5, pp. 1075–1091, 2024.

[6] A. Turner, D. Shieff, A. Dwivedi, and M. Liarokapis, "Comparing machine learning methods and feature extraction techniques for the emg based decoding of human intention," in *2021 43rd Annual International Conference of the IEEE Engineering in Medicine & Biology Society (EMBC)*. IEEE, 2021, pp. 4738–4743.

[7] A. M. Moslhi, H. H. Aly, and M. ElMessiery, "The impact of feature extraction on classification accuracy examined by employing a signal transformer to classify hand gestures using surface electromyography signals," *Sensors*, vol. 24, no. 4, p. 1259, 2024.

[8] H. Li, J. Tang, X. Xu, W. Dai, Y. Liu, J. Xiao, H. Lu, and Z. Zhou, "semg-based gesture-free hand intention recognition: System, dataset, toolbox, and benchmark results," *arXiv preprint arXiv:2411.14131*, 2024.

[9] L. H. Ting and J. L. McKay, "Neuromechanics of muscle synergies for posture and movement," *Current opinion in neurobiology*, vol. 17, no. 6, pp. 622–628, 2007.

[10] A. d'Avella and F. Lacquaniti, "Control of reaching movements by muscle synergy combinations," *Frontiers in computational neuroscience*, vol. 7, p. 42, 2013.

[11] M. F. Rabbi, C. Pizzolato, D. G. Lloyd, C. P. Carty, D. Devaprakash, and L. E. Diamond, "Non-negative matrix factorisation is the most appropriate method for extraction of muscle synergies in walking and running," *Scientific reports*, vol. 10, no. 1, p. 8266, 2020.

[12] K. Zhao, Z. Zhang, H. Wen, B. Liu, J. Li, A. d'Avella, and A. Scano, "Muscle synergies for evaluating upper limb in clinical applications: A systematic review," *Heliyon*, vol. 9, no. 5, 2023.

[13] C. Lv, Y. Liu, Y. Chen, and L. Xie, "semg-based lower limb joint angle prediction with muscle synergy spatio-temporal fusion and dwcit model," *IEEE Sensors Journal*, 2025.

[14] Y. Ma, B. Cui, C. Jiang, H. Gu, H. Zhang, and Q. Zhong, "Extracting muscle synergies using constrained non-negative matrix factorization for motion intention in rehabilitation robotics," in *2024 IEEE International Conference on Robotics and Biomimetics (ROBIO)*. IEEE, 2024, pp. 2383–2387.

[15] P. Qin, X. Shi, C. Zhang, and K. Han, "Continuous estimation of the lower-limb multi-joint angles based on muscle synergy theory and state-space model," *IEEE Sensors Journal*, vol. 23, no. 8, pp. 8491–8503, 2023.

[16] W. Lu, H. Ma, and D. Zeng, "Performance of a novel muscle synergy approach for continuous motion estimation on untrained motion (march 2024)," *IEEE Transactions on Neural Systems and Rehabilitation Engineering*, vol. 32, pp. 3554–3664, 2024.

[17] Y. Zhao, J. Li, J. Zhang, K. Li, D. Wang, H. Li, and J. Zhang, "Personalized gait trajectory prediction of hemiplegic patients based on transfer learning," *IEEE Sensors Journal*, 2025.

[18] Z. Wei, Z. Zhang, and S. Q. Xie, "A transformer framework informed by muscle anatomy and sequence-to-sequence translation for continuous joint kinematics prediction using semg," *IEEE Journal of Biomedical and Health Informatics*, 2025.

[19] J. Huang, Y. Dai, and J. Wang, "Joint angle estimation of lower limb based on pfa-lstm-attention algorithm," in *2023 6th International Conference on Electronics Technology (ICET)*. IEEE, 2023, pp. 1300–1305.

[20] X. Zhou, C. Lin, C. Wang, and X. Peng, "semg-based joint angle estimation via hierarchical spiking attentional feature decomposition network," *IEEE Robotics and Automation Letters*, 2025.

[21] C. Lin and Z. He, "A rotary transformer cross-subject model for continuous estimation of finger joints kinematics and a transfer learning approach for new subjects," *Frontiers in Neuroscience*, vol. 18, p. 1306050, 2024.

[22] G. Du, H. Zhu, Z. Ding, H. Huang, X. Bie, and F. Jiang, "Meta-transfer-learning-based multimodal human pose estimation for lower limbs," *Sensors*, vol. 25, no. 5, p. 1613, 2025.

[23] W. Cao, C. Li, L. Yang, M. Yin, C. Chen, W. Kobsiriphat, T. Utakapan, Y. Yang, H. Yu, and X. Wu, "A fusion network with stacked denoise autoencoder and meta learning for lateral walking gait phase recognition and multi-step-ahead prediction," *IEEE Journal of Biomedical and Health Informatics*, vol. 29, no. 1, pp. 68–80, 2024.

[24] L. Wang, Y. Wang, F. Guo, H. Yan, and F. Zhao, "Lower limb joint angle prediction based on multistream signaling and quantile regression, temporal convolution network–bidirectional long short-term memory network neural network," *Machines*, vol. 12, no. 12, p. 901, 2024.

[25] Z. Wang, H. Chen, F. Yang, X. Wang, X. Wu, and C. Chen, "Accurate prediction of knee joint angles using a hybrid cnn-lstm-attention network from surface electromyography," in *2024 IEEE International Conference on Robotics and Biomimetics (ROBIO)*. IEEE, 2024, pp. 2233–2240.

[26] H. Zhou, S. Zhang, J. Peng, S. Zhang, J. Li, H. Xiong, and W. Zhang, "Informer: Beyond efficient transformer for long sequence time-series forecasting," in *Proceedings of the AAAI conference on artificial intelligence*, vol. 35, no. 12, 2021, pp. 11 106–11 115.

[27] X. Shi, J. Zhang, P. Qin, and R. Liu, "Angle estimation for lower limb joint movement based on vmd-narx algorithm," in *2021 IEEE International Conference on Real-time Computing and Robotics (RCAR)*. IEEE, 2021, pp. 474–479.